

Two Higgs Doublet Model in light of the Standard Model

$H \rightarrow \tau^+\tau^-$ search at the LHC

Abdesslam Arhrib *

Département de Mathématiques, Faculté des Sciences et Techniques, Tanger, Morocco

Department of Physics, National Cheng Kung University, Taiwan 701, Taiwan and

Laboratoire de Physique des Hautes Energies et Astrophysique,

Département de Physiques, Faculté des Sciences Semlalia, Marrakech, Morocco

Cheng-Wei Chiang †

Department of Physics and Center for Mathematics and Theoretical Physics,

National Central University, Chungli 32001, Taiwan

Institute of Physics, Academia Sinica, Taipei 11529, Taiwan and

Physics Division, National Center for Theoretical Sciences, Hsinchu 30013, Taiwan

Dilip Kumar Ghosh ‡

Department of Theoretical Physics, Indian Association for the Cultivation of Science,

2A & 2B Raja S.C. Mullick Road, Kolkata 700 032, India

Rui Santos §

Instituto Superior de Engenharia de Lisboa,

Rua Conselheiro Emídio Navarro 1, 1959-007 Lisboa, Portugal, and

Centro de Física Teórica e Computacional, Faculdade de Ciências,

Universidade de Lisboa Av. Prof. Gama Pinto 2, 1649-003 Lisboa, Portugal.

* aarhrib@ictp.it

† chengwei@ncu.edu.tw

‡ tpdkg@iacs.res.in

§ rsantos@cii.fc.ul.pt

Abstract

We study the implications of the searches based on $H \rightarrow \tau^+\tau^-$ by the ATLAS and CMS collaborations on the parameter space of the two Higgs doublet model (2HDM). In the 2HDM, the scalars can decay into a tau pair with a branching ratio larger than the SM one, leading to constraints on the 2HDM parameter space. We show that in model II, values of $\tan\beta > 1.8$ are definitively excluded if the pseudo-scalar is in the mass range $110 \text{ GeV} < m_A < 145 \text{ GeV}$. We have also discussed the implications for the 2HDM of the recent di-muon search by the ATLAS collaboration for a CP-odd scalar in the mass range 4-12 GeV.

I. INTRODUCTION

The Standard Model (SM) of particle physics has been very successful in explaining most of the experimental observations in elementary particle phenomena. The most crucial and only missing ingredient of the electroweak sector of the SM, the Higgs boson [1, 2], has finally been hinted at CERN's Large Hadron Collider (LHC) by the ATLAS [3, 4] and CMS [5, 6] collaborations. A slight excess was measured both in the $\gamma\gamma$ and in the WW^*, ZZ^* channels, which is compatible with a SM Higgs boson with a mass of about 125 GeV.

Even if a discovery cannot still be claimed, there are well established limits for the SM Higgs. Unitarity of longitudinal weak gauge boson scattering at high energies leads to the bound $M_H \lesssim 700$ GeV [7]. Direct searches of the SM Higgs boson at LEP2 has set a lower bound on the mass $m_H \gtrsim 114.4$ GeV at 95% confidence level (CL) [8]. The CDF and D0 Collaborations at the Tevatron have excluded the Higgs boson mass in the range 156 – 177 GeV at 95% CL [9–11]. The ATLAS and CMS Collaborations have searched for the SM Higgs boson in the $H \rightarrow WW$ channel. The ATLAS Collaboration has excluded the mass range $\sim 155 - 190$ GeV and $\sim 295 - 450$ GeV at 95% CL [12], while the CMS Collaboration has ruled out the Higgs boson mass in the range of $\sim 149 - 206$ GeV and $\sim 300 - 400$ GeV at 95% CL [13]. Very recently, both ATLAS and CMS Collaborations have updated their results on the Higgs boson searches and excluded m_H in the mass ranges [112.7, 115.5] GeV, [131, 237] GeV and [251, 453] GeV for ATLAS [4] and [128, 525] GeV for CMS [6], at 95% CL.

In the SM, a light Higgs decays into a $\tau^+\tau^-$ pair with a branching ratio $\sim 10\%$, which makes it a promising search channel. This channel suffers less from QCD background than the more dominant $b\bar{b}$ channel at the LHC. Moreover, in some versions of models such as the two Higgs doublet model (2HDM), the couplings of the Higgs boson to the third-generation fermions can be strongly enhanced over a large portion of the parameter space; *i.e.*, when $\tan\beta$ is large ($\tan\beta = v_2/v_1$ is the ratio of the two vacuum expectation values (VEV's)). It is therefore useful and timely to constrain such models using this channel. A study for the MSSM using this channel was recently performed in [14]. Searches for Higgs bosons decaying to tau pairs that in turn decay into final states with one or two light leptons at the LHC have been performed by CMS [15] and ATLAS [16] at the CM energy of 7 TeV. Even though the sensitivity of ATLAS and CMS searches has not yet reached the SM sensitivity, useful constraints can be put on new physics model. It is the purpose of this paper to study

the implications of CMS and ATLAS data on the parameters of the 2HDM.

In fact, there are several scenarios in the 2HDM, differing mainly in how the Higgs bosons couple to the SM fermions. One common trend in all scenarios is that the Higgs boson spectrum is the same after electroweak symmetry breaking (EWSB): two charged Higgs particles H^\pm , two CP-even scalars, H, h and one CP-odd scalar, A . By limiting ourselves to natural flavor conservation (NFC), the Higgs couplings to the fermions are completely fixed by α and $\tan\beta$, where α is the mixing angle in the CP-even sector and $\tan\beta$. Therefore, the production rate and decay branching ratios of the Higgs bosons in this model can be worked out readily.

In this paper, we investigate the predictions for the $pp(gg + b\bar{b}) \rightarrow h(A) \rightarrow \tau^+\tau^-$ cross sections and examine the consequences for the 2HDM parameter space. We also discuss the very light CP-odd scenario $m_A \sim 4 - 12$ GeV which decays mainly to a pair of muons for which there are some preliminary results from the ATLAS Collaboration [17].

This paper is organized as follow. In Section II we introduce the patterns of the Yukawa interactions of the 2HDM, while in Section III we illustrate our results for CP-even and CP-odd Higgs bosons which decay to a pair of tau leptons. A discussion of a very light CP-odd scalar decaying to a pair of muons is presented in Section IV. We summarize our findings in Section V.

II. 2HDM AND THE PATTERNS OF THE YUKAWA INTERACTIONS

There are several alternatives to the SM that have started being tested at the LHC. The most popular ones are the Minimal Supersymmetric Standard Model (MSSM) or some of its scalar sector variants like the 2HDMs, little Higgs models and extra dimensions models among others. The 2HDMs are formed by adding an extra complex $SU_L(2) \times U(1)_Y$ scalar doublet with a non-vanishing vacuum expectation value (VEV) to the SM Lagrangian. In the CP-conserving version of 2HDM, we end up with two CP-even scalars, h and H , one CP-odd scalar A and a pair of charged Higgs bosons, H^\pm .

The Yukawa Lagrangian of the 2HDM is a straightforward generalization of the SM one. However, flavor changing neutral currents (FCNC) may occur at tree-level. To avoid tree-level FCNC, it suffices that fermions of a given electric charge couple to no more than one Higgs doublet [18]. It is known that there are four patterns of the Yukawa interaction, free

from tree-level FCNC, depending on the assignment of charges for quarks and leptons under the Z_2 symmetry ($\phi_1 \rightarrow \phi_1$; $\phi_2 \rightarrow -\phi_2$) [19–21]. Hereafter, we define as Type I the model where only the doublet ϕ_2 couples to all fermions; Type II is the model where ϕ_2 couples to up-type quarks and ϕ_1 couples to down-type quarks and charged leptons; in Type III model ϕ_2 couples to up-type quarks and charged leptons and ϕ_1 couples to down-type quarks; the Type IV model is instead built such that ϕ_2 couples to all quarks and ϕ_1 couples to all leptons. Models III and IV have been explored in a number of papers [22–24] and more recently with a renewed interest in [25–27].

	y_h^u	y_h^d	y_h^ℓ	y_A^u	y_A^d	y_A^ℓ
Type-I	$\frac{c_\alpha}{s_\beta}$	$\frac{c_\alpha}{s_\beta}$	$\frac{c_\alpha}{s_\beta}$	$\cot \beta$	$-\cot \beta$	$-\cot \beta$
Type-II	$\frac{c_\alpha}{s_\beta}$	$-\frac{s_\alpha}{c_\beta}$	$-\frac{s_\alpha}{c_\beta}$	$\cot \beta$	$\tan \beta$	$\tan \beta$
Type-III	$\frac{c_\alpha}{s_\beta}$	$-\frac{s_\alpha}{c_\beta}$	$\frac{c_\alpha}{s_\beta}$	$\cot \beta$	$\tan \beta$	$-\cot \beta$
Type-IV	$\frac{c_\alpha}{s_\beta}$	$\frac{c_\alpha}{s_\beta}$	$-\frac{s_\alpha}{c_\beta}$	$\cot \beta$	$-\cot \beta$	$\tan \beta$

TABLE I: Yukawa couplings to the scalars h and A normalized to the SM Higgs Yukawa couplings according to Eq. (1).

After EWSB, the Yukawa interactions of the neutral scalars h and A are expressed in terms of mass eigenstates as:

$$\mathcal{L}_Y^{2HDM} = -\frac{gm_f}{2m_W} y_h^f \bar{f} f h - i \frac{gm_f}{2m_W} y_A^f \bar{f} \gamma_5 f A \quad (1)$$

where the factors $y_{h,A}^f$, needed for this study, are given in Table I in the four Yukawa types of the 2HDM models.

As can be seen from Table I, the models can be grouped in two pairs: (I, IV) and (II, III), as the only difference within each of these two pairs is in the Higgs couplings to the charged leptons. Moreover, the way we have chosen to build the Yukawa Lagrangian is such that up-type quarks have the same couplings to the Higgs bosons in all four types. Down-type quarks have different couplings in the two groups defined above, (I, IV) and (II, III), as can be seen in Table I. In the large $\tan \beta$ limit, in 2HDM-(II, III), the Higgs coupling to a pair of down-type quarks is enhanced by a factor of $1/\cos \beta \approx \tan \beta$ ($\tan \beta \gg 1$), while for 2HDM-(I, IV) there is no such enhancement.

It is well-known that 2HDM parameters can be constrained both from theory and experiment. For example, from perturbativity arguments, the top and bottom Yukawa couplings, $Y_{t,b} = (\frac{g}{\sqrt{2}m_W}\{m_t \cot \beta, m_b \tan \beta\})$, cannot be too large. Therefore, the requirement that $|Y_{t,b}|^2 < 4\pi$ at the tree-level provides a constraint on $\tan \beta$ which reads $0.1 \lesssim \tan \beta \lesssim 100$. Tree-level unitarity [28–30] and vacuum stability [31] also impose severe constraints on the 2HDM parameter space [32]. We note that once a CP-conserving minimum is chosen, the 2HDM is naturally protected against charge and CP-breaking [33–35].

Experimental data and in particular precision data, are now accurate enough to put constraints on new physics models such as the 2HDM's. In this regard, the 2HDM is subject to a number of constraints from which $b \rightarrow s\gamma$, $Z \rightarrow b\bar{b}$, $\delta\rho$, $g-2$ and $B \rightarrow l\nu$ [36–40] are the most relevant. Some of those constraints, such as the ones related to B physics observables, put already some severe constraints on the charged Higgs boson mass and on $\tan \beta$ [36, 37]. Other constraints like $Z \rightarrow b\bar{b}$ [40] and the muon $g-2$ [38, 39] can restrict the available parameter space in the neutral Higgs sector as well. All the above constraints will be taken into account in our analysis.

III. NUMERICAL RESULTS

Before presenting our results, we will discuss the direct experimental constraints on the mass of the lightest CP-even Higgs boson and on the mass of the CP-odd scalar. For the neutral Higgs bosons, the experimental searches depend on the mixing parameters α and $\tan \beta$ and on their decay patterns. If the neutral Higgs bosons decay mainly into fermions, the OPAL, DELPHI and L3 collaborations have set a limit on the masses of h and A in the 2HDM [41, 42]. OPAL claims an exclusion almost independent of the values of α and $\tan \beta$, in the mass ranges $1 \lesssim m_h \lesssim 55$ GeV and $3 \lesssim m_A \lesssim 63$ GeV [41]. It should be noted however that there are several scenarios where the above limits do not hold. First, if either m_h or m_A are above the kinematical threshold in either of the production processes $e^+e^- \rightarrow hZ$ or $e^+e^- \rightarrow hA$, no bound on the masses can be derived. Second, if $\sin(\alpha-\beta) \approx 0$, $\sigma_{e^+e^- \rightarrow hZ} \approx 0$ and again the bound on the CP-even mass do not hold. On the other hand, if $\sin(\alpha-\beta) \approx 1$, $\sigma_{e^+e^- \rightarrow hA} \approx 0$ and in that scenario no bound on the CP-odd mass can be extracted. Assuming that the Higgs-strahlung cross section is the SM one, L3 sets a lower limit on m_h of about 110.3 GeV [41]. Therefore, we will assume from now on that both m_h

and m_A are in the range 110–140 GeV except for a short section where we discuss the case of a very light CP-odd scalar. Regarding the charged Higgs boson, the combined null searches from all four CERN LEP collaborations imply the lower limit $M_{H^\pm} > 78.6$ GeV (95% CL), a limit which applies to all models in which $Br(H^\pm \rightarrow \tau\nu) + Br(H^\pm \rightarrow c\bar{s}) = 1$ [43].

In order to extract limits on the 2HDM parameters, we will focus on the following observables

$$R_\sigma = \frac{\sigma(gg + b\bar{b} \rightarrow \Phi)^{2HDM}}{\sigma(gg + b\bar{b} \rightarrow \Phi)^{SM}}, \quad (2)$$

$$R_{br} = \frac{Br(\Phi \rightarrow \tau\tau)^{2HDM}}{Br(\Phi \rightarrow \tau\tau)^{SM}}, \quad (3)$$

$$R_{\tau\tau} = R_\sigma \times R_{br}, \quad (4)$$

where $\sigma(gg + b\bar{b} \rightarrow \Phi)$ is the production cross section of the scalar particle which has been evaluated at next-to-leading-order (NLO) using HIGLU [44] and bb@nnlo [45] with the CTEQ6 [46] parton distribution function. Note that we include the $b\bar{b}$ fusion contribution since in the 2HDM the $b\bar{b}\phi$ coupling can substantially enhance the production cross section. We will then use the limits obtained by the CMS [15] Collaboration for $R_{\tau\tau}$ at 95% CL.

The decay widths of the scalar particles $\Phi = h, A$ are computed at leading order, both in the SM and in the 2HDM's as

$$\Gamma_\Phi = \sum_{f=\tau,b,c} \Gamma(\Phi \rightarrow ff) + \Gamma(\Phi \rightarrow WW^*) + \Gamma(\Phi \rightarrow ZZ^*) + \Gamma(\Phi \rightarrow gg) + \Gamma(\Phi \rightarrow \gamma\gamma) \quad (5)$$

where the expressions for the scalars decay widths and the respective QCD corrections are taken from [47]. We note that when $\Phi = A$, the decays $\Phi \rightarrow \{WW^*, ZZ^*\}$ are not allowed.

A. CP-odd case

The branching ratio of SM Higgs into $\tau^+\tau^-$ is of the order of 8% for a 100 GeV Higgs boson and drops quickly with an increasing mass. In the 2HDM, $\Phi \rightarrow \tau^+\tau^-$ may be enhanced at large $\tan\beta$, for some types of the 2HDMs under consideration. Such an enhancement can be very large relative to the SM, reaching $\sim 30\%$ in Type II or even 100% in Type IV.

We start by discussing the case of the CP-odd scalar in the 2HDM. Due to CP invariance, A does not couple to WW and ZZ and the partial decay widths to gg and $\gamma\gamma$ are very small. Considering that the channel $A \rightarrow hZ$ is closed, the CP-odd scalar can only decay

into fermions. We have then

$$Br(A \rightarrow \tau\tau) = \frac{\Gamma(\Phi \rightarrow \tau\tau)}{\sum_{f=\tau,b,c} \Gamma(\Phi \rightarrow ff)}. \quad (6)$$

Depending on the Yukawa structure, the above ratio will take different forms which are independent of m_A in the mass region under consideration and can be written as

$$\begin{aligned} Br(A \rightarrow \tau\tau)^I &= \frac{m_\tau^2 \cot \beta^2}{m_\tau^2 \cot \beta^2 + 3m_b^2 \cot \beta^2 + 3m_c^2 \cot \beta^2} \approx 0.075 \\ Br(A \rightarrow \tau\tau)^{II} &= \frac{m_\tau^2 \tan \beta^2}{m_\tau^2 \tan \beta^2 + 3m_b^2 \tan \beta^2 + 3m_c^2 \cot \beta^2} \approx \begin{cases} 0.1 & \text{for } \tan \beta = 100 \\ 0.075 & \text{for } \tan \beta = 1 \end{cases} \\ Br(A \rightarrow \tau\tau)^{III} &= \frac{m_\tau^2 \cot \beta^2}{m_\tau^2 \cot \beta^2 + 3m_b^2 \tan \beta^2 + 3m_c^2 \cot \beta^2} \approx \begin{cases} 10^{-8} & \text{for } \tan \beta = 100 \\ 0.075 & \text{for } \tan \beta = 1 \end{cases} \\ Br(A \rightarrow \tau\tau)^{IV} &= \frac{m_\tau^2 \tan \beta^2}{m_\tau^2 \tan \beta^2 + 3m_b^2 \cot \beta^2 + 3m_c^2 \cot \beta^2} \approx \begin{cases} 1 & \text{for } \tan \beta = 100 \\ 0.075 & \text{for } \tan \beta = 1 \end{cases} \end{aligned} \quad (7)$$

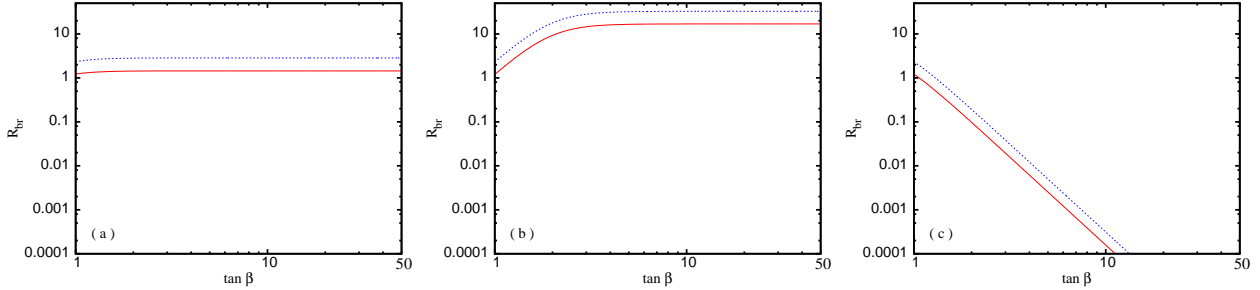


FIG. 1: The ratio R_{br} as a function of $\tan \beta$ for $m_A = 125$ GeV (solid line) and $m_A = 140$ GeV (dashed line) in 2HDM-II, (a) 2HDM-IV (b) and 2HDM-III (c). 2HDM-I is not shown because the $\tan \beta$ dependence drops in this ratio.

As one can see, in terms of branching ratios, we can have an enhancement in $Br(A \rightarrow \tau\tau)$ in the 2HDM with respect to the SM, which can be quantified by R_{br} , in the following cases:

- 2HDM-II with large $\tan \beta$: $Br(A \rightarrow \tau\tau)^{II} \approx 1.2 \times Br(H \rightarrow \tau\tau)^{SM}$,
- 2HDM-IV with large $\tan \beta$: $Br(A \rightarrow \tau\tau)^{IV} \approx 13 \times Br(H \rightarrow \tau\tau)^{SM}$.

It should be noted that values of $\tan \beta < 1$ are already excluded by the precision constraints in the 2HDM. In Fig. 1, we present the ratio R_{br} as a function of $\tan \beta$ for $m_A = 125$ GeV (solid line) and $m_A = 140$ GeV (dashed line) in 2HDM-II (a), 2HDM-IV (b) and 2HDM-III

(c). The 2HDM-I scenario is not shown because the $\tan \beta$ dependence in this ratio cancels out.

Let us now turn to the ratio R_σ . The A and h couplings to $b\bar{b}$ are proportional to $\tan \beta$ for large $\tan \beta$ in Types II and III, as shown in Table I. Therefore, for large $\tan \beta$ only those models can present an enhancement in the cross section coming from the bottom loop in the gluon fusion process and from $b\bar{b}$ fusion. The only difference between A and h is in the mixing angle $\sin \alpha$ which is present in all Yukawa couplings and will be discussed in the next section. In Fig. 2 we present R_σ as a function of $\tan \beta$ for $m_A = 125$ GeV (solid line) and

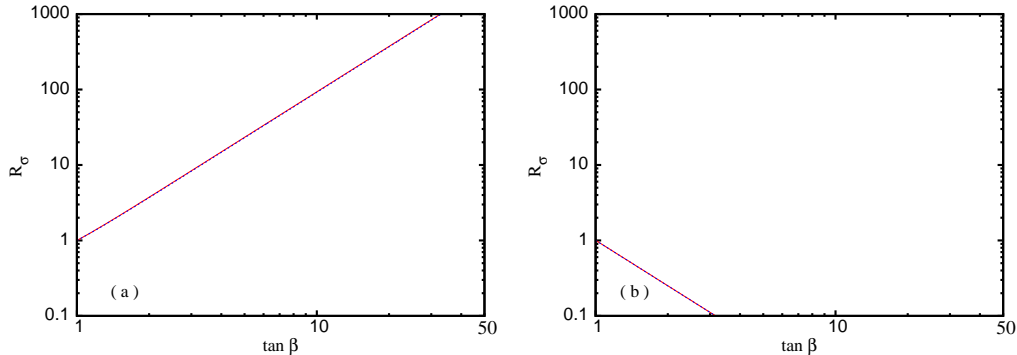


FIG. 2: The ratio R_σ as a function of $\tan \beta$ for $m_A = 125$ GeV (solid line) and $m_A = 140$ GeV (dashed line) in 2HDM-II, III (a) and 2HDM-I,IV (b).

$m_A = 140$ GeV (dashed line) in 2HDM-II, IV (a) and 2HDM-I,III (b). It is clear that an enhancement relative to the SM can only be obtained for large $\tan \beta$ and just for 2HDM-II and III.

It is now easy to understand the values of $R_{\tau\tau}$ presented in Fig. 3 as a function of $\tan \beta$ for $m_A = 125$ GeV (solid line) and $m_A = 140$ GeV (dashed line). The horizontal lines in the figures indicate the CMS 95% CL lower limit for $m_A = 125$ GeV (lower line) and $m_A = 140$ GeV (upper line) [15]. In 2HDM-II (Fig. 3(b)), for a given CP odd Higgs boson mass, there is just a small window of $\tan \beta$ which is allowed by the CMS data on $R_{\tau\tau}$. It is clear that, for 2HDM-II, values of $\tan \beta \geq 2$ are definitely excluded at 95% CL for the entire mass range under scrutiny. In 2HDM-IV, the excluded region reduces to a tiny window centred at $\tan \beta = 2$, while for 2HDM-I and III $\tan \beta$ is allowed in the entire range shown.

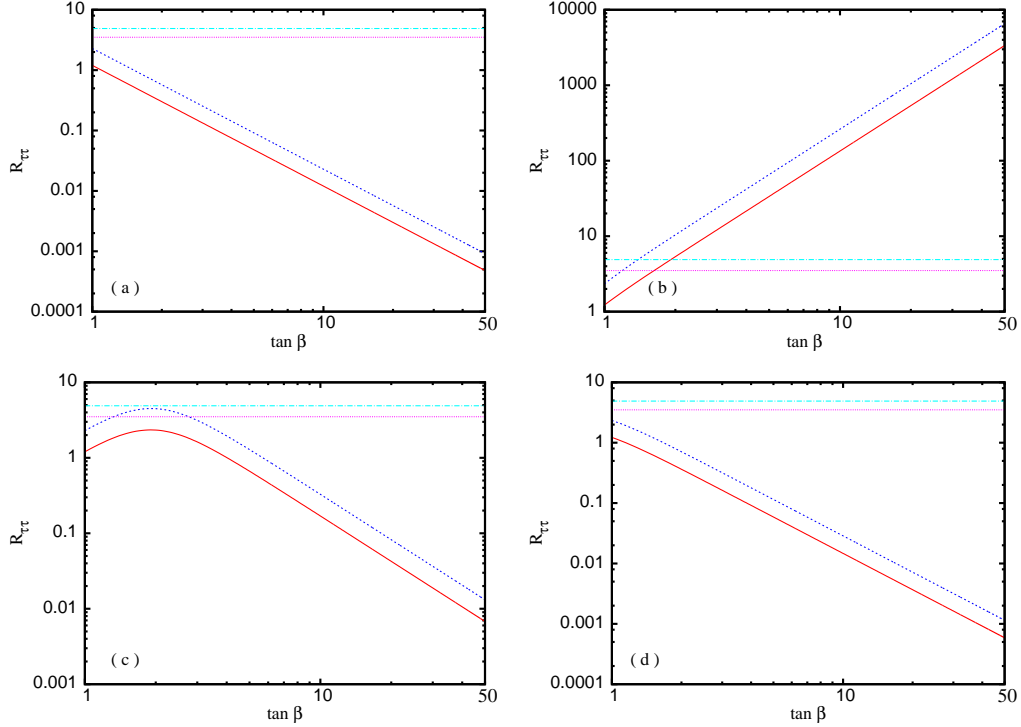


FIG. 3: The ratio $R_{\tau\tau}$ as a function of $\tan\beta$ for $m_A = 125$ GeV (solid line) and $m_A = 140$ GeV (dashed line) in 2HDM-I, (a), 2HDM-II (b), 2HDM-IV, (c), and 2HDM-III (d). The horizontal lines indicate the 95% CL CMS [15] lower limit for $m_A = 125$ GeV (lower line) and $m_A = 140$ GeV (upper line).

B. CP-even case

We will now move on to the study of the lightest CP-even scalar. Although similar, the process $pp(gg + b\bar{b}) \rightarrow h \rightarrow \tau^+\tau^-$, is in fact more evolved since the Yukawa couplings of h depend both on $\tan\beta$ and α . Throughout this section we take $\sin\alpha > 0$ to make the plots clearer. There is an approximate symmetry in the values of $R_{\tau\tau}$ between positive and negative values of $\sin\alpha$. In the final exclusion plots, we will allow $\sin\alpha$ to vary in the entire range from -1 to 1 though. We shall now discuss each Yukawa model in turn.

1. 2HDM-I

In 2HDM-I, all fermions couple to h proportionally to $y_h^\tau = y_h^b = y_h^c = \frac{\cos\alpha}{\sin\beta}$. Such a Higgs would be fermiophobic in the limit $\cos\alpha = 0$ ($\sin\alpha = \pm 1$) where the production cross section would be reduced. Since $\tan\beta > 1$, R_σ is approximately constant in all $\tan\beta$ range as shown

in Fig. 4 (middle) where R_σ is shown as a function of $\tan\beta$ for several values of $\sin\alpha$ and $m_h = 125$ GeV.

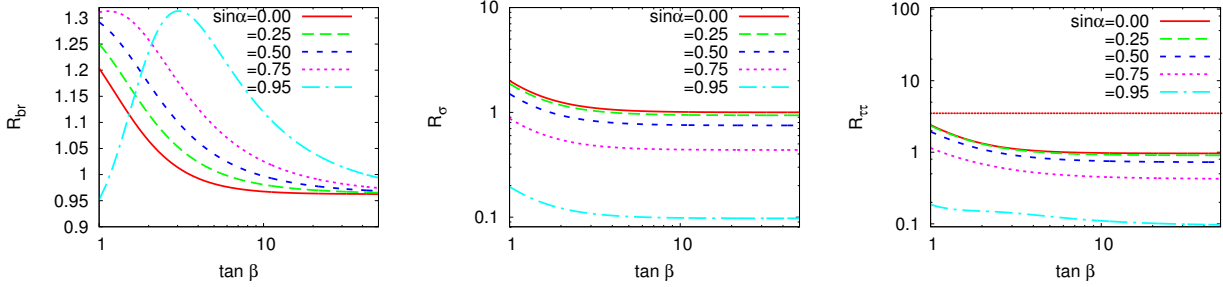


FIG. 4: R_{br}^h , R_σ and $R_{\tau\tau}$ as functions of $\tan\beta$ for several values of $\sin\alpha$ with $m_h = 125$ GeV in 2HDM-I. The horizontal dotted line indicates the 95% CL CMS lower limit on $R_{\tau\tau}$ for $m_h = 125$ GeV.

The branching ratio of the CP-even Higgs boson, h , to the $\tau\tau$ mode takes the following form

$$Br(h \rightarrow \tau\tau) = \frac{m_\tau^2 (y_h^\tau)^2}{m_\tau^2 (y_h^\tau)^2 + 3m_b^2 (y_h^b)^2 + 3m_c^2 (y_h^c)^2 + F(\Gamma_{WW^*}, \Gamma_{ZZ^*})}, \quad (8)$$

where $F(\Gamma_{WW^*}, \Gamma_{ZZ^*})$ is proportional to the partial widths of $h \rightarrow WW^*$ and $h \rightarrow ZZ^*$, and the former is about $0.2 \Gamma_{Total}^{SM}$ for a Higgs boson of 125 GeV. Since $y_h^\tau = y_h^b = y_h^c$ in 2HDM-I, this common factor will cancel out in the branching ratio formula Eq. (8), rendering a $Br(h \rightarrow \tau\tau)^I$ similar to the corresponding SM rate. This is illustrated in Fig. 4 (left), where we can see that the ratio R_{br} is close to one except for some modulations due to the $h \rightarrow WW^*$ contribution, which is proportional to $\sin(\beta - \alpha)$. At large $\tan\beta$, the contribution of the vector bosons decays lose their angular dependence, amounting to a reduction in $Br(h \rightarrow \tau\tau)^I$ as shown in Fig. 4 (left).

From the above discussions, one can readily understand the shape of $R_{\tau\tau}$ in 2HDM-I presented in Fig. 4 (right). $R_{\tau\tau}$ is almost independent of $\tan\beta$ in the entire range shown and decreases with increasing $\sin\alpha$ due to the cross section behaviour. It is also clear from the plots that there are no excluded regions in the 2HDM-I parameter space from the recent LHC data on $R_{\tau\tau}$.

2. 2HDM-II

In 2HDM-II, as seen in Table I, the h couplings to a pair of τ leptons and to $b\bar{b}$ are proportional to $y_h^\tau = y_h^b = \frac{\sin\alpha}{\cos\beta}$. These couplings will boost the $b\bar{b} \rightarrow h$ cross section at high $\tan\beta$ as compared to the SM one. The h coupling to top-quarks is proportional to $y_h^u = \frac{\cos\alpha}{\sin\beta}$. This implies that the top loop in the $gg \rightarrow h$ cross section could only be enhanced at small $\tan\beta$, while for large $\tan\beta$ the bottom loop will take over.

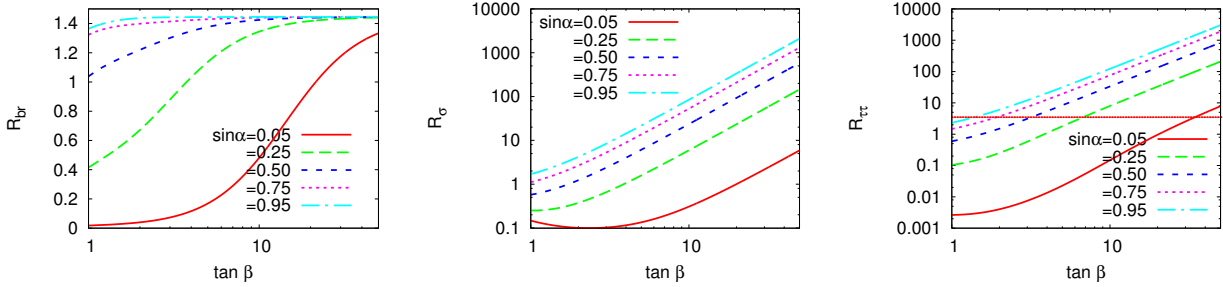


FIG. 5: R_{br}^h , R_σ and $R_{\tau\tau}$ as a function of $\tan\beta$ for several values of $\sin\alpha$ with $m_h = 125$ GeV in the 2HDM-II. The horizontal dotted line indicates the 95% CL CMS lower limit on $R_{\tau\tau}$ for $m_h = 125$ GeV.

In 2HDM-II, a large $\tan\beta$ does modify significantly the branching ratio of $h \rightarrow \tau^+\tau^-$ relative to the SM one. The only possible enhancement factor, $1/\cos\beta$ [Eq. (8)] will cancel amongst the main fermion contributions. Therefore, $R_{br} \approx 1.4$ for large $\tan\beta$ as can be read from Fig. 5 (left). When $\tan\beta$ is small, the branching ratio of $h \rightarrow \tau^+\tau^-$ is suppressed. This suppression is even more pronounced for smaller $\sin\alpha$ and when $\sin\alpha \rightarrow 0$, $Br(h \rightarrow \tau^+\tau^-) \rightarrow 0$ and consequently $R_{br} \rightarrow 0$.

On the other hand, the production cross section via both gluon and $b\bar{b}$ fusion is enhanced with respect to the SM Higgs production rate for large $\tan\beta$ and not too small $\sin\alpha$, as can be seen in Fig. 5 (middle).

Finally, the ratio $R_{\tau\tau}^{II}$ is shown in Fig. 5 (right). Taking into account the dotted line of the 95% CL CMS lower limit on $R_{\tau\tau}$ for $m_h = 125$ GeV we conclude that a substantial part of the $\tan\beta$ range presented is excluded, except for very small values of $\sin\alpha$.

3. 2HDM-III

In 2HDM-III, the h couplings to a pair of fermions are proportional to $y_h^\tau = y_h^c = \frac{\cos \alpha}{\sin \beta}$, $y_h^b = \frac{-\sin \alpha}{\cos \beta}$. Therefore, as in model II, the bottom Yukawa coupling will be enhanced for large $\tan \beta$. As $\tan \beta$ increases, the partial width of the $h \rightarrow b\bar{b}$ becomes large and thus suppresses $Br(h \rightarrow \tau^+\tau^-)$. This is illustrated in Fig. 6 (left), where the role played by $\sin \alpha$ is clearly observed. Of course for $\sin \alpha = 0$, $h \rightarrow b\bar{b}$ vanishes and $Br(h \rightarrow \tau^+\tau^-)$ is at least more than 2 times larger than the SM rate for almost all values of $\tan \beta$.

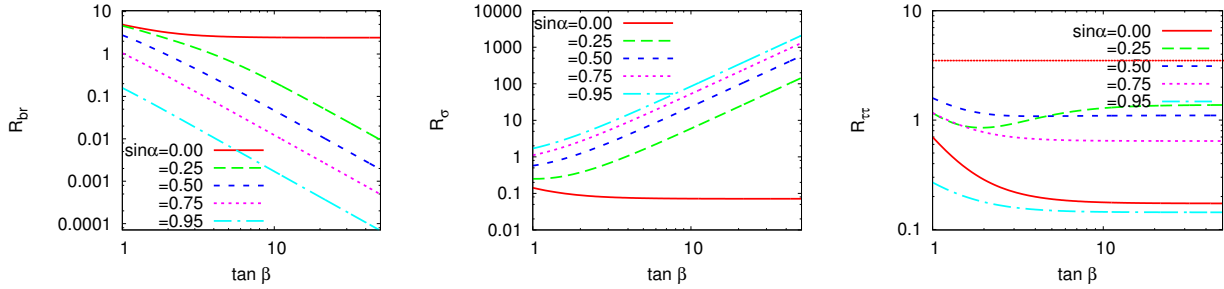


FIG. 6: R_{br}^h , R_σ and $R_{\tau\tau}$ as functions of $\tan \beta$ for several values of $\sin \alpha$ with $m_h = 125$ GeV in 2HDM-III. The horizontal dotted line indicates the 95% CL CMS lower limit on $R_{\tau\tau}$ for $m_h = 125$ GeV.

In Fig. 6 (middle), we see the enhancement of the cross section at large $\tan \beta$ due to the b-quark loop and the $b\bar{b}$ production cross section. However, once combined with R_{br} , the ratio $R_{\tau\tau}$ is always well below the CMS lower limit at 95% CL. Therefore the entire range of $\tan \beta$ is allowed, independently of the values of $\sin \alpha$.

4. 2HDM-IV

In 2HDM-IV (also known as the lepton-specific model), the h couplings to a pair of fermions are $y_h^\tau = \frac{-\sin \alpha}{\cos \beta}$ and $y_h^b = y_h^c = \frac{\cos \alpha}{\sin \beta}$, relative to the SM ones. Hence, only y_h^τ can be enhanced relative to the SM at large $\tan \beta$. As stated previously, in 2HDM-IV the $Br(h \rightarrow \tau^+\tau^-)$ can be 100% at large $\tan \beta$ and not too small $\sin \alpha$. This can be seen in Fig. 7 (left), where R_{br} can reach values slightly larger than 10.

As for model I, the production cross section relative to the SM are almost independent of $\tan \beta$ for the entire range presented in in Fig. 6 (middle). There is however a $\sin \alpha$

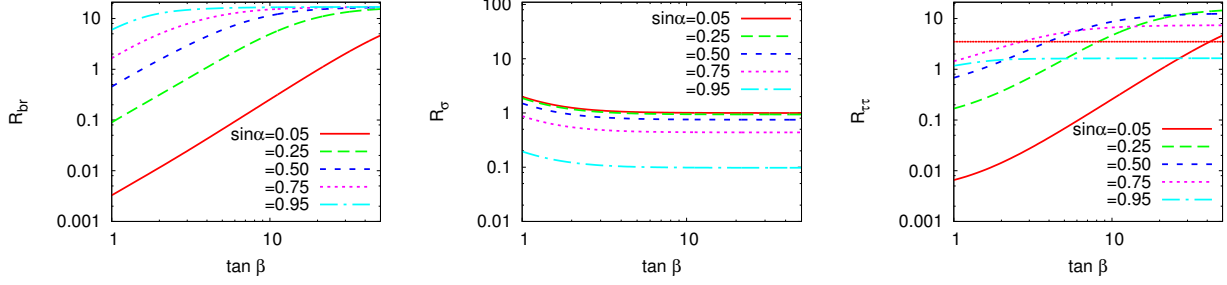


FIG. 7: R_{br}^h , R_{σ} and $R_{\tau\tau}$ as functions of $\tan \beta$ for several values of $\sin \alpha$ with $m_h = 125$ GeV in 2HDM-IV. The horizontal dotted line indicates the CMS limit for $m_h = 125$ GeV.

dependence: R_{σ} decreases with increasing $\sin \alpha$. When $\sin \alpha \rightarrow 1$, it is clear that the production cross section will vanish since $y_h^b = y_h^c$ is proportional to $\cos \alpha \rightarrow 0$.

The ratio $R_{\tau\tau}^{IV}$ is shown in Fig. 6 (right). At large $\tan \beta$, we can see the effect of the R_{br} enhancement. The excluded region depends heavily on $\sin \alpha$ and will be presented in the conclusions.

IV. A VERY LIGHT CP-ODD BOSON

A very light CP-odd Higgs boson is not excluded in the proposed 2HDM ¹. In fact, the LEP bounds on the 2HDM parameters based on the $e^+e^- \rightarrow hA$ [43] production process, do not hold if either $\sin(\beta - \alpha) \approx 1$ or if the mass of the lightest Higgs is such that the production is either disallowed or its rate is very small. However, LEP has also produced bounds that depend solely on the Yukawa couplings of the models.

There were searches at LEP based on the Yukawa processes $e^+e^- \rightarrow b\bar{b}A \rightarrow b\bar{b}\tau^+\tau^-$ in the mass range $m_A = 4 - 12$ GeV [50] and in the channels $b\bar{b}b\bar{b}$, $b\bar{b}\tau^+\tau^-$, $\tau^+\tau^-\tau^+\tau^-$ for pseudoscalar masses up to 50 GeV [42]. These bounds on the Yukawa couplings can be divided into three groups: bounds on $g_{A\tau^+\tau^-}^2$, $g_{A\bar{b}b}^2$ and $g_{A\bar{b}b} g_{A\tau^+\tau^-}$. In 2HDM-I, we have $g_{A\tau^+\tau^-}^2 = g_{A\bar{b}b}^2 = g_{A\bar{b}b} g_{A\tau^+\tau^-} = 1/\tan^2 \beta$ and, consequently, a lower bound on $\tan \beta$ can be extracted. In model type II, the relation is $g_{A\tau^+\tau^-}^2 = g_{A\bar{b}b}^2 = g_{A\bar{b}b} g_{A\tau^+\tau^-} = \tan^2 \beta$ and, therefore, an upper bound on $\tan \beta$ can be obtained as a function of the CP-odd scalar mass. Finally in models type III and IV, no bounds on $\tan \beta$ can be derived in the mass region

¹ Some attentions have been recently given to the very low CP-odd Higgs boson mass region, decaying into muons, in the next-to-Minimal Supersymmetric Model [48, 49]

$m_A = 4 - 12$ GeV because $g_{A\bar{b}b} g_{A\tau^+\tau^-} = 1$.

Recently, the ATLAS Collaboration has searched for a very light CP-odd scalar [17] in the mass region 4 – 12 GeV with the process $pp \rightarrow A \rightarrow \mu^+\mu^-$. As previously discussed, the cross section for the production of a CP-odd particle can only increase for large $\tan\beta$ in models type II and III — the top quark couples to the CP-odd scalar proportionally to $1/\tan\beta$, while the bottom quark couples proportionally to $\tan\beta$ in those scenarios. On the other hand, the largest possible value for $Br(A \rightarrow \mu^+\mu^-)$ arises in Type IV while in Type III the branching ratio to fermions is negligible for large $\tan\beta$. Therefore, in the high $\tan\beta$ region, one would expect to reach the highest possible values for $\sigma(pp \rightarrow A \rightarrow \mu^+\mu^-)$ in Types II and IV. Note that when one moves to values of $\tan\beta$ below 1, the top-quark loop dominates in the production process that is similar in all scenarios. As the ATLAS result pertains only to the mass region 4 – 12 GeV, we can only compare their result with those obtained by the OPAL Collaboration [50].

m_A (GeV)	4	5	6	7	8	9	10	11	12
$\tan\beta_{Br(A\rightarrow\tau^+\tau^-)=100\%}^{II}$	8.5	11.0	9.6	11.5	10.7	11.0	11.3	12.3	13.6
$\tan\beta^{II}$	≈ 8.5	≈ 11.0	≈ 9.6	≈ 11.5	≈ 10.7	> 100	> 100	> 100	> 100

TABLE II: Bounds from the OPAL Collaboration on $\tan\beta$ for Type II with m_A varying between 4 to 12 GeV. The second line shows the limits assuming $Br(A \rightarrow \tau^+\tau^-) = 100\%$. The last line in the table takes into account the actual values of $Br(A \rightarrow \tau^+\tau^-)$ in Type II.

The OPAL results are shown in Table II in the form of a limit on $\tan\beta$ as a function of the scalar mass. In the second line of the table the limits assume $Br(A \rightarrow \tau^+\tau^-) = 100\%$, while in the last line the actual values of $Br(A \rightarrow \tau^+\tau^-)$ for Type II are taken into account. Using the ATLAS result on $pp \rightarrow A \rightarrow \mu^+\mu^-$, we can now inquire whether the bounds on $\tan\beta$ for $m_A = 4 - 12$ GeV are improved relative to the OPAL bounds. In our calculation, we do not take into account the appearance of bound states.

Before proceeding further, it should be mentioned that there is a very constraining experimental bound from the muon $(g-2)_\mu$ [38, 39, 51, 52]. A detailed account on the subject can be found in Ref. [53]. Including new physics contributions from the 2HDM will be performed by taking off the diagrams where the SM Higgs boson takes part and adding the new physics contributions; that is, $\Delta a_\mu = (a_\mu^{exp} - a_\mu^{th-SM}) + a_\mu^{th-2HDM}$. The two most

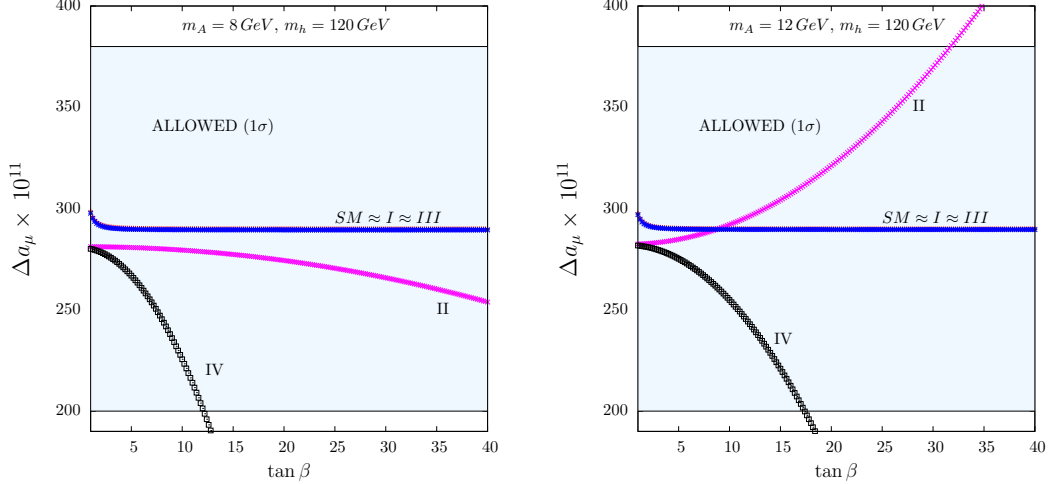


FIG. 8: The left panel shows $\Delta a_\mu = (a_\mu^{exp} - a_\mu^{th-SM}) + a_\mu^{th-2HDM}$ as a function of $\tan \beta$ for $m_A = 8$ GeV and $m_h = 120$ GeV in the limit $\alpha \approx \beta$. The same is for the right panel except $m_A = 12$ GeV. The other 2HDM parameters do not contribute to $a_\mu^{th-2HDM}$.

important contributions from extended models to the muon anomalous magnetic moment are the one-loop contribution, first calculated for the 2HDM in Ref. [54], and the two-loop Barr-Zee contribution [55]. While the one-loop contribution is proportional to $g_{h\mu^+\mu}^2$ and has therefore the SM sign, the two-loop contribution is either proportional to $g_{h\mu^+\mu} g_{h\bar{b}b}$ or to $g_{h\mu^+\mu} g_{h\bar{t}t}$ and can therefore have either sign in the 2HDM. As a result, the one-loop contribution helps curing the 3σ deviation relative to the SM, while the two-loop contribution can, if sufficiently large, increase or decrease the difference between theory and experiment. In Fig. 8, we present $\Delta a_\mu = (a_\mu^{exp} - a_\mu^{th-SM}) + a_\mu^{th-2HDM}$ as a function of $\tan \beta$ for $m_h = 120$ GeV and $m_A = 8$ GeV (left) and $m_A = 12$ GeV (right) in the limit $\alpha \approx \beta$. The other 2HDM parameters do not contribute to $a_\mu^{th-2HDM}$. It is clear from the plots that it is possible to accommodate the contributions from the 2HDM within the 1σ bound even for very low m_A masses. The most striking feature is, however, the dependence on the CP-odd scalar: a small change in the mass can lead to a big change in its contribution to the muon anomalous magnetic moment.

Taking into account the Yukawa couplings, only Types II and IV are worth further exploration. However, it turns out that for model IV, all parameter space is allowed although values of $\tan \beta \approx 2$ are close to being excluded. In the left panel of Fig. 9 we present the cross section for $pp \rightarrow A \rightarrow \mu^+\mu^-$ in 2HDM-II as a function of the pseudo-scalar mass

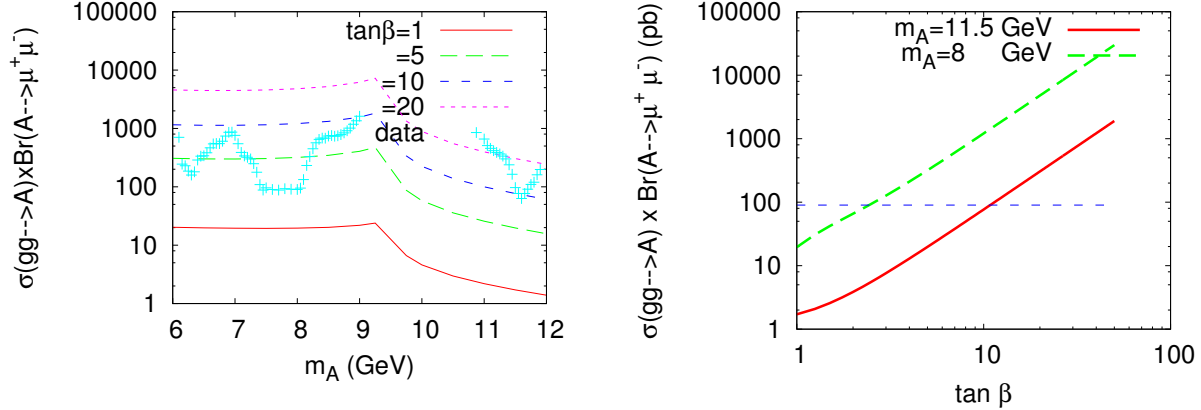


FIG. 9: In the left panel we show the $pp \rightarrow A \rightarrow \mu^+\mu^-$ cross section in 2HDM-II as a function of the pseudo-scalar mass for several values of $\tan\beta$ together with the observed limits on $\sigma(pp \rightarrow A \rightarrow \mu^+\mu^-)$ taken from ATLAS [17]. In the right panel we present $pp \rightarrow A \rightarrow \mu^+\mu^-$ in 2HDM-II as a function of $\tan\beta$ for $m_A = 8$ GeV (dashed line) and $m_A = 11.5$ GeV (full line). The dashed horizontal line represents the experimental limit [17]. Limits on $\tan\beta$ are the points where the theoretical cross section intersects with the dashed experimental line.

for several values of $\tan\beta$ together with the observed limits on $\sigma(pp \rightarrow A \rightarrow \mu^+\mu^-)$ taken from ATLAS [17]. In the right panel of Fig. 9 we show $pp \rightarrow A \rightarrow \mu^+\mu^-$ in 2HDM-II as a function of $\tan\beta$ for $m_A = 8$ GeV (dashed line) and $m_A = 11.5$ GeV (full line). The dashed horizontal line represents the experimental limit [17]. Limits on $\tan\beta$ are the points where the theoretical cross section intersects with the dashed experimental line. The lines intersect at $\tan\beta \approx 2.4$ for $m_A = 8$ GeV and $\tan\beta \approx 14.5$ for $m_A = 10.9$ GeV. When compared with the bounds obtained by the OPAL Collaboration, we conclude that below the $\bar{b}b$ threshold the results are better than the ones obtained with the OPAL data. Above the $\bar{b}b$ threshold, the results would be competitive with the DELPHI ones had they done the analysis for scalar masses below 12 GeV. Since this did not happen, results for the mass region between 11 and 12 GeV are the first ones to put a strong limit on $\tan\beta$ for Type II. For the reasons already discussed, no limits can be extracted for the remaining Yukawa types of the model.

V. CONCLUSIONS

The very recent results from the CMS and ATLAS Collaborations on the search for neutral Higgs bosons decaying to tau pairs at $\sqrt{s} = 7$ TeV has prompted us to analyze its implications for CP-conserving 2HDM's with natural flavor conservation. From the four possible Yukawa types of the model, we have concluded that for only two of them the experimental constraints result in relevant exclusion regions in the 2HDM parameter space. This conclusion already takes into account the fact that other experimental constraints have already excluded the $\tan \beta < 1$ region.

We now summarize the results for $\tan \beta > 1$ in the four scenarios, starting with the CP-even Higgs boson. In Type I, the branching ratios are very similar to the SM ones while the production cross section is always below the SM rate. Model III has an increased cross section relative to the SM, yet the branching ratio to a tau pair is much smaller due to the $\tan \beta$ dependence. Hence, the ratio $R_{\tau\tau}$ is always below 1 for Type I and Type III. In Fig. 10, we show the exclusion region for $m_h = 125$ GeV in the $(\tan \beta, \sin \alpha)$ plane. In the left panel for Type II, the allowed region shrinks as one moves to large values of $|\sin \alpha|$. For $\sin \alpha \approx 0$, all values of $\tan \beta$ are allowed. In the right panel for Type IV, both regions of small and large $|\sin \alpha|$ are now allowed. If we believe the 125 GeV Higgs boson hinted at by the $\gamma\gamma$ measurements, then the large values of $|\sin \alpha|$ are excluded [56].

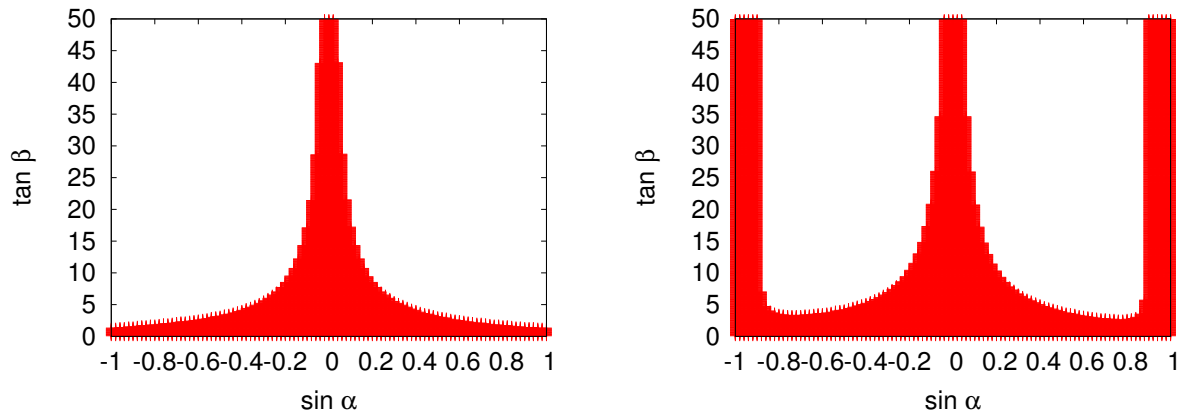


FIG. 10: Exclusion plots by $pp \rightarrow h \rightarrow \tau^+\tau^-$ in the $(\tan \beta, \sin \alpha)$ plane for $m_h = 125$ GeV in 2HDM-II (left) and 2HDM-IV (left). Red color areas are not excluded.

The CP-odd scalar analysis leads to a similar conclusion with the bonus that the parameter $\sin \alpha$ is not relevant. The results are presented in the $(\tan \beta, m_A)$ plane. Again, for

$\tan\beta > 1$ no interesting exclusion can be found for Type I, Type III and now also for Type IV. As stated previously, values of $\tan\beta \approx 2$ are close to being excluded in Type IV, and more data will possibly exclude some window centred at $\tan\beta = 2$. In Fig. 11, we show the results for Type II where the exclusion region is quite large. In fact, for all values of the CP-odd scalar mass, values of $\tan\beta > 1.8$ are definitively excluded. Taking into account that $\tan\beta$ is already constrained to be above 1, the present results are close to exclude all values of $\tan\beta$ if the pseudo-scalar is in the mass range considered. The study recently performed in [57] concludes that if the excess observed at the LHC comes from $A \rightarrow \gamma\gamma$, $\tan\beta \approx O(1)$, which is still allowed within experimental and theoretical errors in all four models.

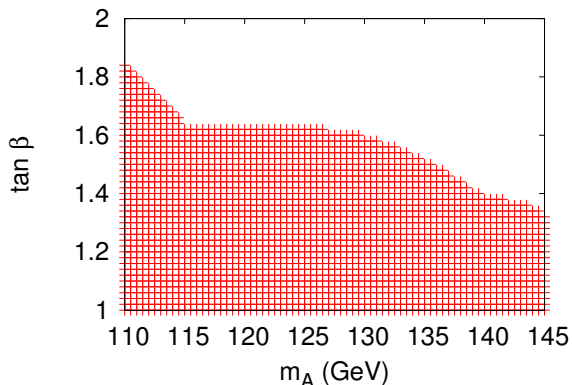


FIG. 11: Exclusion plot by $pp \rightarrow A \rightarrow \tau^+\tau^-$ in the $(\tan\beta, m_A)$ plane in 2HDM-II. Values above $\tan\beta = 2$ are excluded in Type II.

Acknowledgments

A. A. acknowledges the support from NSC under contract # 100-2811-M-006-008. C.-W. C. is supported in part by NSC Grant No. 100-2628-M-008-003-MY4 and NCTS. D. K. G. acknowledges partial support from the Department of Science and Technology, India under the grant SR/S2/HEP-12/2006. He would also like to thank the ICTP High Energy Group, Trieste for their hospitality, where part of this work was done. R. S. is supported in part by the Portuguese *Fundação para a Ciência e a Tecnologia* (FCT) under contracts PTDC/FIS/117951/2010 and PEst-OE/FIS/UI0618/2011 and by an FP7 Reintegration

- [1] P. W. Higgs, Phys.Lett. **12**, 132 (1964).
- [2] F. Englert and R. Brout, Phys.Rev.Lett. **13**, 321 (1964).
- [3] The ATLAS collaboration, ATLAS-CONF-2011-161 (2011).
- [4] The ATLAS collaboration, ATLAS-CONF-2011-163 (2011).
- [5] The CMS collaboration, CMS-PAS-HIG-11-030 (2011).
- [6] The CMS collaboration, CMS-PAS-HIG-11-032 (2011).
- [7] B. W. Lee, C. Quigg, and H. Thacker, Phys.Rev. **D16**, 1519 (1977).
- [8] R. Barate et al. (LEP Working Group for Higgs boson searches, ALEPH Collaboration, DELPHI Collaboration, L3 Collaboration, OPAL Collaboration), Phys.Lett. **B565**, 61 (2003), hep-ex/0306033.
- [9] T. Aaltonen et al. (The CDF Collaboration), Phys.Rev.Lett. **104**, 061803 (2010), 1001.4468.
- [10] V. Abazov et al. (The D0 Collaboration), Phys.Rev.Lett. **104**, 061804 (2010), 1001.4481.
- [11] T. Aaltonen et al. (CDF and D0) (2011), 1103.3233.
- [12] K. Cranmer (ATLAS Collaboration, EPS-HEP 2011, July 21 -27, 2011; Grenoble, Rhone-Alpes France) (2011).
- [13] A. Koryton (CMS Collaboration, EPS-HEP 2011, July 21 -27, 2011; Grenoble, Rhone-Alpes France) (2011).
- [14] J. Baglio and A. Djouadi (2011), 1103.6247.
- [15] The CMS collaboration, CMS-PAS-HIG-11-029 (2011).
- [16] G. Aad et al. (ATLAS) (2011), 1107.5003.
- [17] The ATLAS collaboration, ATLAS-CONF-2011-020 (2011).
- [18] S. L. Glashow and S. Weinberg, Phys. Rev. **D15**, 1958 (1977).
- [19] V. D. Barger, J. L. Hewett, and R. J. N. Phillips, Phys. Rev. **D41**, 3421 (1990).
- [20] Y. Grossman, Nucl. Phys. **B426**, 355 (1994), hep-ph/9401311.
- [21] A. G. Akeroyd and W. J. Stirling, Nucl. Phys. **B447**, 3 (1995).
- [22] R. M. Barnett, G. Senjanovic, and D. Wyler, Phys. Rev. **D30**, 1529 (1984).
- [23] R. M. Barnett, G. Senjanovic, L. Wolfenstein, and D. Wyler, Phys. Lett. **B136**, 191 (1984).
- [24] H.-S. Goh, L. J. Hall, and P. Kumar, JHEP **05**, 097 (2009), 0902.0814.

- [25] S. Su and B. Thomas, Phys. Rev. **D79**, 095014 (2009), 0903.0667.
- [26] H. E. Logan and D. MacLennan, Phys. Rev. **D79**, 115022 (2009), 0903.2246.
- [27] M. Aoki, S. Kanemura, K. Tsumura, and K. Yagyu, Phys. Rev. **D80**, 015017 (2009), 0902.4665.
- [28] S. Kanemura, T. Kubota, and E. Takasugi, Phys.Lett. **B313**, 155 (1993), hep-ph/9303263.
- [29] A. G. Akeroyd, A. Arhrib, and E.-M. Naimi, Phys.Lett. **B490**, 119 (2000), hep-ph/0006035.
- [30] J. Horejsi and M. Kladiva, Eur.Phys.J. **C46**, 81 (2006), hep-ph/0510154.
- [31] N. G. Deshpande and E. Ma, Phys.Rev. **D18**, 2574 (1978).
- [32] M. Aoki et al., Phys. Rev. **D84**, 055028 (2011), 1104.3178.
- [33] P. Ferreira, R. Santos, and A. Barroso, Phys.Lett. **B603**, 219 (2004), hep-ph/0406231.
- [34] M. Maniatis, A. von Manteuffel, O. Nachtmann, and F. Nagel, Eur.Phys.J. **C48**, 805 (2006), hep-ph/0605184.
- [35] I. Ivanov, Phys.Rev. **D75**, 035001 (2007), hep-ph/0609018.
- [36] A. Wahab El Kaffas, P. Osland, and O. M. OGREID, Phys. Rev. **D76**, 095001 (2007), 0706.2997.
- [37] F. Mahmoudi and O. Stal, Phys. Rev. **D81**, 035016 (2010), 0907.1791.
- [38] K. Cheung and O. C. W. Kong, Phys. Rev. **D68**, 053003 (2003), hep-ph/0302111.
- [39] K.-m. Cheung, C.-H. Chou, and O. C. W. Kong, Phys. Rev. **D64**, 111301 (2001), hep-ph/0103183.
- [40] H. E. Haber and H. E. Logan, Phys. Rev. **D62**, 015011 (2000), hep-ph/9909335.
- [41] G. Abbiendi et al. (OPAL), Eur. Phys. J. **C40**, 317 (2005), hep-ex/0408097.
- [42] J. Abdallah et al. (DELPHI), Eur. Phys. J. **C38**, 1 (2004), hep-ex/0410017.
- [43] S. Schael et al. (ALEPH), Eur. Phys. J. **C47**, 547 (2006), hep-ex/0602042.
- [44] M. Spira (1995), hep-ph/9510347.
- [45] R. V. Harlander and W. B. Kilgore, Phys.Rev. **D68**, 013001 (2003), hep-ph/0304035.
- [46] P. M. Nadolsky et al., Phys. Rev. **D78**, 013004 (2008), 0802.0007.
- [47] A. Djouadi, Phys. Rept. **457**, 1 (2008), hep-ph/0503172.
- [48] R. Dermisek and J. F. Gunion, Phys. Rev. **D81**, 055001 (2010), 0911.2460.
- [49] M. M. Almarashi and S. Moretti, Phys. Rev. **D83**, 035023 (2011), 1101.1137.
- [50] G. Abbiendi et al. (OPAL), Eur. Phys. J. **C23**, 397 (2002), hep-ex/0111010.
- [51] M. Krawczyk and J. Zochowski, Phys. Rev. **D55**, 6968 (1997), hep-ph/9608321.
- [52] A. Dedes and H. E. Haber, JHEP **05**, 006 (2001), hep-ph/0102297.

- [53] F. Jegerlehner and A. Nyffeler, Phys. Rept. **477**, 1 (2009), 0902.3360.
- [54] H. E. Haber, G. L. Kane, and T. Sterling, Nucl. Phys. **B161**, 493 (1979).
- [55] S. M. Barr and A. Zee, Phys. Rev. Lett. **65**, 21 (1990).
- [56] P. M. Ferreira, R. Santos, M. Sher, and J. P. Silva (2011), 1112.3277.
- [57] G. Burdman, C. Haluch, and R. Matheus (2011), 1112.3961.